ROLE OF SENSITIVITY ANALYSIS IN DETERMINING REACTOR QUANTITIES

By

K. MIHÁLY

Nuclear Training Reactor of the Technical University, Budapest

Received: February 18, 1982
Presented by Dir. Dr. GY. CSOM

1. Introduction

The problem involved in showing the relationship between deterministic and random phenomena cannot be avoided if we wish to describe or predict a phenomenon properly. A phenomenon, an event, can be described the more satisfactorily the less 'space' we leave for random factors.

It is possible to overcome the difficulties of decreasing or eliminating random factors but this can only be done if we are able to reveal the boundary between the deterministic and random factors in the phenomenon itself.

Reactor physics describes the deterministic behaviour of neutrons in a real reactor through a solution of the transport equation yielding the average flux. The effect of randomness is here realized in the uncertainty of the input data.

The method of solving the transport equation is developed to such an extent that it can, in principle, be considered accurate; moreover, this is valid — within given error limits — for the approximate methods too. These error limits of the approximate methods are determined in magnitude and sign, and if we compare the results obtained against more accurate calculation methods then revision is possible using correction factors. Such correction eliminates the errors of the calculation methods, but it means that the calculation model is not adequate for actual reactors.

The situation is different concerning the correction of the random error deriving from the uncertainty of the input data. This error is mainly due to:

— the wide technological tolerances of the different constructional units of the reactor.

— errors arising from constants, because of the inaccuracy of the nuclear data and neutron cross sections used for reactor calculations.

The answer to the problem of inaccuracy of the cross section data is that they are derived from out-of-reactor experiments and they thus contain all kinds of measuring errors and correlation properties of various origins.

If we wish to demonstrate the measuring difficulties from nuclear cross section data we need only refer to the fact that thousands of physicists in

laboratories all over the world have been working on this topic since 1940. Such a huge amount of data has accumulated that nowadays these data are deals with by an international organization.

Currently, this organization has four regional neutron data centres: the National Neutron Cross Section Centre (NNCS) in Brookhaven, USA; the Centre de Compilation de Données Neutroniques (CCDN) in Saclay, France; the Nunclear Data Section (NDS) in Vienna, Austria; and the Centr po Jadernüm Dannüm (CJD) in Obninsk, USSR. Their publication, CINDA* forms a categorized system containing millions of estimated data and references based on several million experimental results.

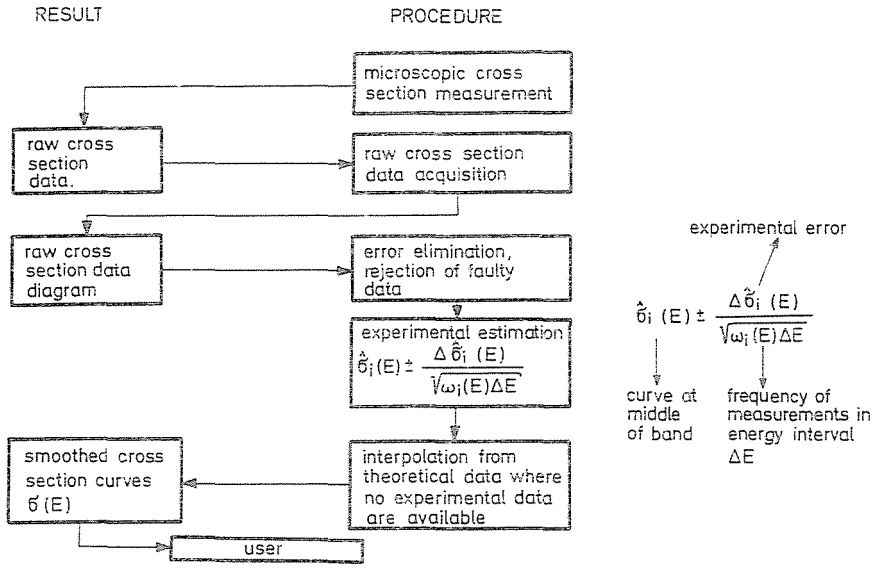

Fig. 1

Based on the compilation of the cross section data it can be pointed out that the cross section data for a given energy frequently differ more from each other than the standard deviation assigned to the corresponding measurements. In view of this, it is not sufficient just to collect the cross section data they must also be estimated. A flow-chart of an estimation procedure resulting in optimal cross section data is shown in Fig. 1.

The cross section tables and diagrams prepared for the purpose of reactor calculations generally contain smoothed curves $\sigma(E)$. If the values belonging to

* The Computer Index of Neutron Data, exchanged between the four regional neutron data centres.

these 'recommended' curves are changed to a small extent compared with their standard deviation or their estimated uncertainty, this may result in a significant change in the reactor quantities for reactor calculations. This statement can also be formulated as follows: new information can be obtained for cross section data if reactor quantities are determined through experiments that can be measured more accurately than the cross section data concerned.

2. Determination of reactor quantities

Our present investigations cover the so-called extensive or integral quantities; we will also refer to these as reactor quantities. It is characteristic to reactor quantities that their values depend also on the size and shape of the reactor. Such reactor quantities are: critical size, critical mass, effective multiplication factor (k_{eff}), shielding factor, energy spectrum, spectral indices, etc. The values of these quantities measured in critical systems have been utilized since 1964 to make cross sections more accurate [1]. It has become apparent that the calcuation accuracy required in reactor design cannot be reached by using cross section data measured out of the reactor that have not been improved by integral experiments performed within the reactor. Naturally, such an approach to the question could only be realized and widely accepted on the basis of the results of the intensive theoretical and experimental research that has been carried out internationally since 1964 [2–10].

The application of cross section data made more accurate by reactor quantities can be summarized in the following steps:

1. Determination of the selected reactor quantity by integral measurement;
2. Selection of an appropriate nuclear cross section data set;
3. Execution of transport calculations using the selected data set to determine the integral quantity;
4. Comparison of the measured and calculated values of the integral quantity;
5. Determination of the simultaneous optimum values of the reactor quantity obtained from the integral measurement and that of the cross section;
6. Fitting of the cross section data, re-calculation of the reactor quantity with the fitted data set. The reactor quantity calculated with the fitted data set should result in a better agreement with the measured values.

The procedure outlined in the above six steps presupposes that

— during the fitting, and for better agreement between calculated and measured values of the reactor quantity, it is not permitted for an improvement on the cross section to be so large that the improved value falls outside the error limits of the experimental value;

— the difference between the calculated and measured value of the reactor quantity may only derive from experimental statistical errors of the nuclear cross section data and not from errors in the calculation model or systematic or other errors.

3. Cross section sensitivity analysis in biological shield calculations

The intensity of the interaction between neutrons and nuclei of the shielding material can be given numerically if, for example, activation reaction rate is determined on the basis of the measured values of the activation detectors. The reaction rate is an integral property of the neutrons passing through the shield and, as an integral property, it enables the cross section correction procedure employed for core calculations to be extended to biological shield calculations. This question is comprehensively treated by Goldstein [11].

Integral quantities measured at different points in different biological shielding configurations at the Training Reactor of the Technical University of Budapest are discussed on the basis of the procedure described in the previous section.

The measured values of the integral quantities are taken from ref. [12]. The integral quantity is the reaction intensity of neutron activation determined on the basis of the measured values of the indium (In), gold (Au) and sulphur (S) activation detectors at the marked points in the four different configurations shown in Fig. 2 [12].

The nuclear data set ABBN [13] was selected as a means of calculating the measured integral quantity — the reactor quantity.

When choosing the calculation method, it had to be considered that it should be capable — in a problem-oriented way — of solving the stationary kinetic equation describing the neutron transport in the shielding material, i.e. the distribution of neutrons with respect to space, energy and angle [14]:

$$\bar{\Omega}\nabla\Phi(\bar{r}, E, \bar{\Omega}) + \sum_t(\bar{r}, E)\Phi(\bar{r}, E, \bar{\Omega}) = \\ = \int \mathrm{d}\Omega' \int \mathrm{dE}'\, \Phi(\bar{r}, E', \bar{\Omega})\, W(\bar{r}, \mu_0, E' \to E) + q(\bar{r}, E, \bar{\Omega}), \tag{1}$$

where

$\Phi(\bar{r}, E, \bar{\Omega})$ is the neutron flux characterized by the velocity vector of direction $\bar{\Omega}$ and energy E at point r;

Σ_t the total macroscopic cross section;

$W(\bar{r}, \mu_0, E' \to E)$ number of neutrons scattered from point $(\bar{\Omega}, E')$ to point $(\bar{\Omega}, E)$;

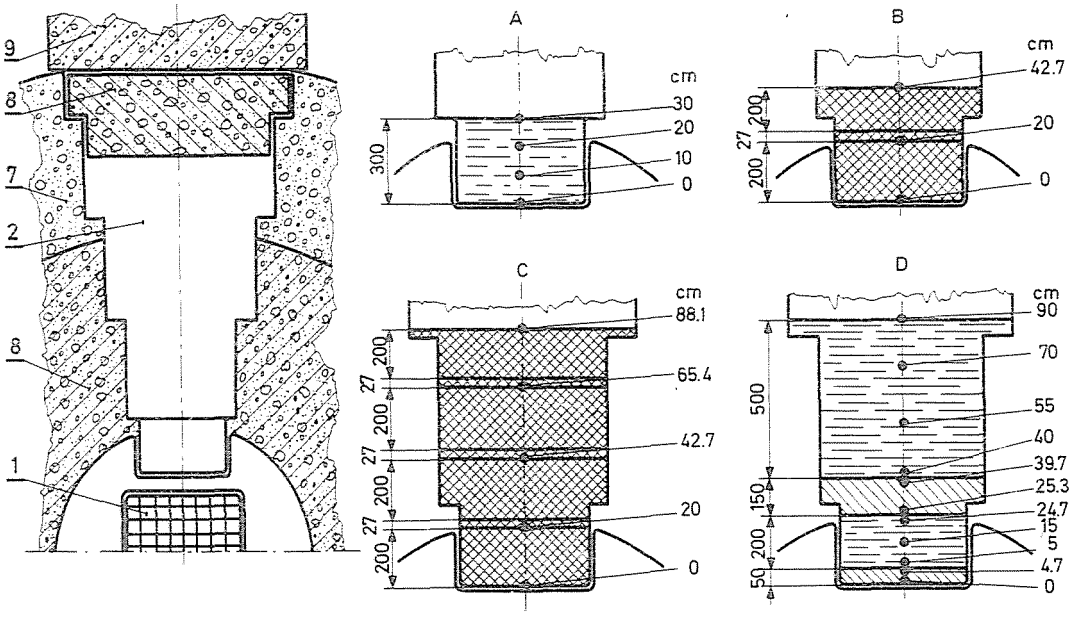

Fig. 2. Shielding configuration patterns in the irradiation channel of the Training Reactor T. U. Budapest; 1. reactor core 2. irradiation channel 7. normal concrete 8. heavy concrete 9. concrete door; A. Configuration 1,30 cm water slab. B. Configuration 2,40 cm graphite-layer. C. Configuration 3,80 cm graphite-layer. D. Configuration 4, sandwich-shield

$\mu_0 = \Omega \cdot \bar{\Omega}' = \cos \nu_0$ cosine of the scattering angle of neutrons in the laboratory system;

$q(\bar{r}, E, \bar{\Omega})$ intensity of the fission neutron source characterized by the velocity vector of direction $\bar{\Omega}$, emerging with energy E at point r.

To solve the transport equation, Eq. (1), we used the removal-diffusion approximation method [15]; our reasons for this are given below.

In the present case the transport calculations were for a hydrogen-containing medium so the calculation method should not alter the physical properties of the interaction process between the neutron and the nucleus. It is known that in a laboratory system this interaction is characterized by strong anisotropic scattering and a large energy loss per collision. The deep penetration activity of neutrons, so decisive in biological shielding calculations, cannot be described by a calculation model (such as Fermi age theory) that takes no account of the correlation in the scattering angle and the large energy loss for each collision. The removal-diffusion method, on the other hand overcomes all these difficulties and it has the additional advantage that complicated calculation procedures can also be avoided by its use.

The curve of the neutron cross section referring to hydrogen is given in Fig. 3. It can be seen in the figure that the value of the scattering cross section

σ_s^H, in function of the energy eV, is relatively high and virtually independent of the energy at low and medium energies. For high energies, a monotonic decrease in the cross section curve can be observed as a function of increasing energy values. The small value of σ_s^H beyond 1 MeV and the slowing down below 1 MeV lead to the appearance of the deep penetrating component in the neutron spectrum. In the case of a fission spectrum this refers to neutrons with an approximate energy of 8 MeV.

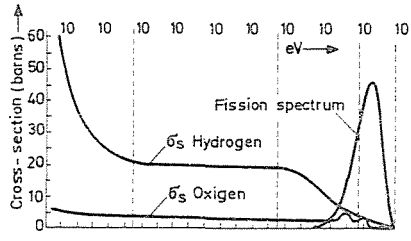

Fig. 3. Neutron cross section in hydrogen

The transport of deep penetrating neutrons takes place along nearly bee-line orbits, i.e. in the form of small angle elastic scatterings.

Because of the inelastic collisions entailing a considerable energy loss, the large angle elastic scatterings, and the 'mingling' of neutrons with the medium, a certain number of neutrons are 'knocked-out' of or removed from the deep penetrating component, and the multiple collisions of these 'knocked-out' neutrons form the slowing down neutron spectrum. This spectrum forms at the site of the generation of the neutrons; the spatial distribution of the neutrons is followed by the distribution of the deep penetrating component, especially with large shielding thicknesses.

Based on the above, the following statements are valid: a neutron spectrum forms in hydrogen-containing media at a certain distance from the external neutron source that can arbitrarily be divided into two components. The first of these is a deep penetrating component comprising fast neutrons; this components is responsible for the spatial distribution of the neutrons. The second component is represented by the slowing down neutrons which thus influence the shape of the neutron spectrum mainly.

Let us consider the matter mathematically and take the neutron flux in Eq. (1) to be the sum of two arbitrary components: $\varphi+\psi$. Here, φ is the contribution of the multiple scattered neutrons to the flux, i.e. the slowing down component; ψ is the contribution of the neutrons without or with small angle scatteinrg to the flux, i.e. the deep penetrating component.

If it is assumed that the slowing down neutrons show isotropic scattering Eq. (1) can be written as a system of two equations, viz.

$$\bar{\Omega}\nabla\psi(\bar{r}, E)+\Sigma_B(\bar{r}, E)\,\psi(\bar{r}, E)=q(\bar{r}, E);$$

$$-D\Delta\varphi(\bar{r}, E)+\Sigma_t\varphi(\bar{r}, E)= \tag{2}$$

$$=\int\varphi(\bar{r}, E')\,W(\bar{r}, E'\to E)+Q(\bar{r}, E).$$

Here

$q(\bar{r}, E)$ is the intensity of the fission source of neutrons emerging with energy E;

$Q(\bar{r}, E)$ the distributed source of neutrons slowed down to energy E which can be given by the following relationship:

$$Q(\bar{r}, E)=\int\psi(\bar{r}, E')\,\Sigma_B(\bar{r}, E'\to E)\,\mathrm{d}E,$$

where $\psi(\bar{r}, E')\,\Sigma_B(\bar{r}, E'\to E)$ is the number of scattered neutrons:

$\Sigma_B(\bar{r}, E)$ is the removal-diffusion cross section which is considered as the difference between the total cross section describing the interaction between the neutrons and the nuclei and the elastic cross section giving the small solid-angle forward-scattering.

Equation system (2) was solved by means of the MBD code [16] for all four shielding configurations in Fig. 2. The results of the calculations were published in ref. [17]. The calculation model was checked by a more sensitive transport theoretical approach, the so-called integral equation method, and the results were published in ref. [18]. The calculated results of both methods were compared with each other and with the results from ref. [12]. The calculated results show the average deviation of the measured and calculated reactor quantitites to be 30%.

The reaction rate value for configurations 1 and 2, calculated by the removal-diffusion method described above are given in Table 1 together with the measured values taken from ref. [12]; the deviation between the calculated and measured values is also displayed.

To achieve the best possible agreement between the calculated and measured values of a reactor quantity, we need to analyse the cross section sensitivity.

Analysis of this sort examines how a reactor quantity is sensitive to the variations in a given set of cross section data, i.e. we are interested in the response of the reactor quantity to the perturbation of the cross section. Consequently, the derivative of the integral quantity versus the cross section must be determined, from which the sensitivity profile can then be obtained.

Table 1

Results calculated with removal-diffusion MBD code compared with experimental results

	[cm] (according to Fig. 2.)	In-detector			S-detector		
		E > 1 MeV			E > 3 MeV		
		Reaction rate [$cm^{-3} s^{-1}$]			Reaction rate [$cm^{-3} s^{-1}$]		
	[cm] (from Fig. 2.)	Measured*	Calculated	Calculated / Measured	Measured*	Calculated	Calculated / Measured
CONFIG 1	0	$1.78 \cdot 10^7$	$1.156 \cdot 10^7$	0.649	$6.59 \cdot 10^6$	$3.690 \cdot 10^6$	0.560
	10	$3.08 \cdot 10^6$	$2.332 \cdot 10^6$	0.757	$1.33 \cdot 10^6$	$9.344 \cdot 10^5$	0.703
	20	$7.07 \cdot 10^5$	$6.644 \cdot 10^5$	0.940	$2.81 \cdot 10^5$	$3.040 \cdot 10^5$	1.082
	30**	$2.04 \cdot 10^5$	$3.050 \cdot 10^5$	1.495	$7.61 \cdot 10^4$	$1.450 \cdot 10^5$	1.905
CONFIG 2	0	$2.18 \cdot 10^7$	$1.977 \cdot 10^7$	0.907	$7.87 \cdot 10^6$	$5.368 \cdot 10^6$	0.682
	20	—	$3.319 \cdot 10^6$	—	$1.06 \cdot 10^6$	$8.546 \cdot 10^5$	0.806
	42.7	$2.74 \cdot 10^5$	$3.597 \cdot 10^5$	1.313	$1.06 \cdot 10^5$	$1.053 \cdot 10^5$	0.993

* results from ref. [12]

** The considerable deviation in the measured and calculated reaction intensity values at this coordinate point is caused by the back scattering by the concrete door, in consequence of which the values measured at points near to the door are higher than the calculated ones. The measured and calculated results for the 30 cm water slab in configuration 1 and the last 50 cm of the water slab of the sandwich-shield in configuration 4 are displayed together in Fig. 4. It can be seen from the figure that the measured values at the 30 cm point of configuration 1 and at the 50 cm point of configuration 4 (this latter corresponds to the 90 cm point in Fig. 2) scatter toward the calculated values; this is especially conspicuous at the measured value of $2.28 \cdot 10^6$ $cm^{-3} s^{-1}$ related to the 50 cm point. At the same time, however, the trend of the calculated curves is the same for both configurations — which one might expect from the physical picture

Two methods are available to determine the sensitivity profile: the variations of the cross section for each group (ref. [6]), and the method of adjoint differential equations (ref. [22]) based on perturbation theory [20, 21]. Even though the second method seems to have been more in the focus of interest lately (refs. [11] [23–25]), we rejected it for two reasons. The first is that the sensitivity profile can be obtained in linear approximation by the method based on linear perturbation theory. It is known, however, that the sensitivity profile is noticeably not a linear function (see ref. [11]) for the cross section perturbations calculated with an experimental error of about 5–10%. The second and main reason stems from the difficulty in constructing the adjoint operator in the case of the removal-diffusion method due to the semi-empirical nature of the method.

Thus, opting for the method of variation of cross section we proceeded first to determine the group fluxes for the given configurations by the removal-diffusion method with unperturbed cross section data and then, from these, the reaction rates based on the values measured by the detectors. The cross section

data concerned were then decreased by 10% consecutively for each group, and recalculation was then performed with these data according to the first step. In the present case the cross sections concerned are the total cross sections of the oxygen and carbon, and the perturbation of 10% was chosen because of the error characterizing the group cross section data.

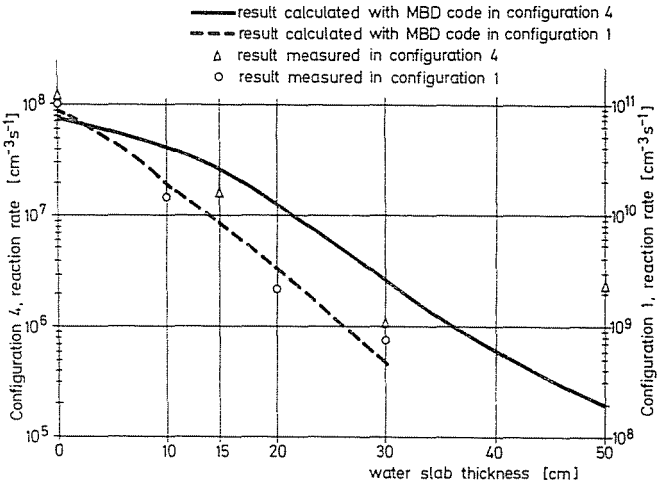

Fig.4 Comparison of measured and calculated reaction rate values in water shield

Configuration 4	Configuration 1
$7.389 \cdot 10^7$ △ $1.17 \cdot 10^8$	$8.81 \cdot 10^{10}$ ○ $1.08 \cdot 10^{11}$
$2.389 \cdot 10^7$ △ $1.71 \cdot 10^7$	$1.78 \cdot 10^{10}$ ○ $1.40 \cdot 10^{10}$
$2.807 \cdot 10^6$ △ $1.10 \cdot 10^6$	$3.50 \cdot 10^9$ ○ $2.19 \cdot 10^9$
$2.165 \cdot 10^5$ △ $2.28 \cdot 10^6$	$5.25 \cdot 10^8$ ○ $8.24 \cdot 10^8$

The calculations were carried out in all the 26 energy groups by the method described, for each activation detector and all measuring points. The sensitivity profile was constructed by the formula:

$$R_i = \left(\frac{I_0 - I_i}{I_i} \Big/ \frac{\Delta\sigma}{\sigma} \right) \cdot \frac{1}{\Delta\mu_i}, \tag{3}$$

where

I_0 is the detector response by the unperturbed cross section;

I_i the detector response in the i-th group with 10% decrease of the total cross section;

$\frac{\Delta\sigma}{\sigma} (= -10\%)$ relative cross section variation;

$\Delta\mu_i$ group width in lethargy units.

It should be noted that during the sensitivity analysis, the cross section data are distorted by strongly correlated statistical errors. The combined effect of these errors should be taken into account at the correct determination of the error of the functional.

If the group cross section data are independent of each other then the total sensitivity can be calculated from the formula

$$R = \sqrt{\sum_i R_i^2}\,, \tag{4}$$

where R_i is the sensitivity referring to the i-th group cross section.

It is mentioned that the 26-group ABBN data set [13] used in our calculations was estimated from a huge amount of correlated experimental cross section data, similarly to the procedure shown in Fig. 1. Consequently, expression (4) is an under-estimation. Since we have no accurate values for the correlation matrix elements, the following quantity is defined for estimating the total sensitivity:

$$R = \sum_i |R_i| \tag{5}$$

which means the upper limit of sensitivity [26].

The sensitivity profiles were calculated by the above-mentioned method for the possible combinations of the following quantities:

perturbed cross sections: — oxygen and carbon;
integral quantities: — reaction rate (from the responses of In, Au and S detectors),
— integral neutron flux,
— dose rate;
shield thickness calculation sites: 0, 10, 17, 22, 24, 27, 32, 40 (shield thickness and the measuring point corresponding to these sites can be seen in Figs 7 and 8).

The calculated results were published in ref. [19]. In the present paper only sensitivity data calculated for configurations 1 and 2 are given in Tables 2 and 3. As an example, two sensitivity profiles are presented in Figs 5 and 6, based on the data of Tables 2 and 3.

Sensitivity analysis enables the following statements to be made:

a.) It holds for all activation detectors that they are not sensitive to variation in cross section in the low energy range. This is true, of course, not only where the value of the cross section is zero but also in an energy range

Table 2

Neutron flux activation sensitivity for group cross section variation
Configuration 1

In $E>1$ MeV

Calculation node points (See Fig. 7.)						
Group number	10	17	22	27	32	40
1	0.0	0.0092	−0.0178	−0.0887	−0.1980	−0.3634
2	0.019	0.0636	−0.0535	−0.3289	−0.7525	−1.2612
3	0.0194	0.0909	−0.1426	−0.3550	−0.5446	−0.3634
4	0.0163	0.0051	−0.1051	−0.1539	−0.1751	−0.0630
5	0.0	0.0153	−0.0300	−0.0220	−0.0167	0.0
6	0.0	0.0032	−0.0124	−0.0036	0.0	0.0
7			0			
⋮						
26			0			
$\sum_{j=1}^{26} =$	0.0547	0.2473	−0.3614	−0.9521	−1.6869	−2.0511

S $E>3$ MeV

1	0.0055	0.0127	−0.0454	−0.1732	−0.3370	−0.5285
2	0.0166	0.1021	−0.1323	−0.4762	−0.9317	−1.2914
3	0.0110	0.0766	−0.1488	−0.2814	−0.3766	−0.1990
4	0.0	0.0107	−0.0209	−0.0273	−0.0334	−0.0116
5			0			
⋮						
26			0			
$\sum_{j=1}^{26} =$	0.0331	0.2021	−0.3473	−0.9581	−1.6787	−2.0305

differing from zero (see, for example, at the Au detector). This means that sensitivity analysis is of no use for cross section improvement, and that the method employing the removal-diffusion code does not require very accurate cross section data in this range.

b.) The sensitivity in absolute value increases with increasing shield thickness, i.e. for a thicker shield the uncertainty of the group cross section data cannot be ignored.

The total sensitivity is demonstrated in Figs. 7 and 8 for oxygen and carbon cross section variations, for each activation detector versus the thickness of water and graphite shield, based on the values of Tables 2 and 3.

(Table 2 continued)

Au $0.5 < E < \infty$ eV

Group number	Calculation node points (See Fig. 7)					
	10	17	22	27	32	40
1	0.0052	0.0	0.0	−0.0289	−0.1158	−0.2869
2	0.0052	0.0099	0.0074	−0.1445	−0.6942	−1.0500
3	0.0104	0.0199	−0.0149	−0.2282	−0.4741	−0.5088
4	0.0131	0.0252	−0.0688	−0.2384	−0.3250	−0.1869
5	0.0087	0.0168	−0.0688	−0.1022	−0.0650	−0.0046
6	0.0072	0.0135	−0.0465	−0.0442	−0.0230	0.0
7	0.0036	0.0069	−0.0258	−0.0181	−0.0115	0.0
8	0.0036	0.0069	−0.0155	−0.0080	−0.0038	0.0
9	0.0032	0.0062	−0.0093	−0.0036	−0.0034	0.0
10	0.0032	0.0	−0.0046	−0.0018	−0.0034	0.0
11	0.0032	0.0	−0.0046	−0.0018	−0.0034	0.0
12	0.0032	0.0	−0.0046	−0.0018	−0.0034	0.0
13	0.0032	0.0	−0.0046	−0.0018	−0.0034	0.0
14	0.0032	0.0062	−0.0046	−0.0018	0.0	0.0
15	0.0032	0.0062	−0.0046	−0.0018	0.0	0.0
16	0.0032	0.0062	−0.0046	−0.0018	0.0	0.0
17	0.0032	0.0062	−0.0046	−0.0018	0.0	0.0
18	0.0032	0.0062	−0.0046	−0.0018	−0.0034	0.0
19	0.0032	0.0062	−0.0046	−0.0018	−0.0034	0.0
20	0.0032	0.0124	−0.0046	0.0090	0.0034	0.0
21	0.0	0.0	−0.0278	−0.0234	−0.0172	0.0
22	0.0	0.0	−0.0046	−0.0018	−0.0034	0.0
23	0.0	0.0	0.0	0.0	0.0	0.0
24	0.0	0.0	0.0	0.0	0.0	0.0
25	0.0	0.0	0.0	0.0	0.0	0.0
26	0.0	0.0	0.0	0.0	0.0	0.0
$\sum_{j=1}^{26} =$	0.09540	0.1553	−0.3252	−0.8503	−1.7534	−2.0370

(Table 2 continued)

Au $0 < E < \infty$ eV

Group number	Calculation node points (See Fig. 7)					
	10	17	22	27	32	40
1	0.0	0.0	0.0	−0.0119	−0.0580	−0.2782
2	0.0046	0.0076	0.029	−0.0595	−0.2515	−1.0363
3	0.0046	0.0076	−0.0029	−0.0950	−0.2708	−0.5140
4	0.0078	0.0064	−0.0123	−0.1001	−0.2118	−0.1937
5	0.0039	0.0064	−0.0197	−0.0501	−0.0597	−0.0048
6	0.0032	0.0053	−0.0122	−0.0248	−0.0269	−0.0020
7	0.0032	0.0	−0.0061	−0.0165	−0.0135	0.0
8	0.0032	0.0	−0.0041	−0.0083	−0.0045	0.0
9	0.0029	0.0	−0.0018	−0.0074	−0.0040	0.0
10	0.0	0.0	−0.0018	0.0	0.0	0.0
11	0.0	0.0	−0.0018	0.0	0.0	0.0
12	0.0	0.0	−0.0018	0.0	0.0	0.0
13	0.0	0.0	−0.0018	0.0	0.0	0.0
14	0.0	0.0	−0.0018	0.0	0.0	0.0
15	0.0	0.0	−0.0018	0.0	0.0	0.0
16	0.0	0.0	−0.0018	0.0	0.0	0.0
17	0.0	0.0	−0.0018	0.0	0.0	0.0
18	0.0	0.0	−0.0018	0.0	0.0	0.0
19	0.0	0.0	−0.0018	0.0	0.0	0.0
20	0.0	0.0	−0.0018	0.0	0.0	0.0
21	0.0	0.0	−0.0036	0.0	−0.0040	0.0
22	0.0	0.0	−0.0018	0.0	0.0	0.0
23	0.0	0.0	−0.0018	0.0	0.0	0.0
24	0.0	0.0	−0.0018	0.0	0.0	0.0
25	0.0	0.0	−0.0018	0.0	0.0	0.0
26	0.0174	0.0427	−0.0748	−0.1483	−0.2331	0.0
$\sum_{j=1}^{26} =$	0.0508	0.0760	−0.13550	−0.5219	−1.138	−2.029

Table 3

Neutron flux activation sensitivity for group cross section variation
Configuration 2

In $E>1$ MeV

Calculation node points (See Fig. 7)					
Group number	10	17	24	32	40
1	0.01779	0.0176	−0.0692	−0.3958	−1.0700
2	0.03560	0.0941	−0.5076	−2.7022	−5.3398
3	0.01780	0.0353	−0.9344	−1.7050	−0.8365
4	0.0	−0.0473	−1.0977	−2.1986	−0.0434
5	0.0	−0.0446	−0.3206	−0.4359	0.0
6	0.0	−0.0164	−0.0802	−0.0953	0.0
7	0.0	−0.0020	−0.0080	−0.0106	0.0
8			0		
⋮					
26			0		
$\sum_{j=1}^{26} =$	0.07119	0.0367	−3.0177	−7.5434	−7.2897

S $E>3$ MeV

1	0.0052	0.0192			
4	−0.0052	−0.0323	−0.3750	−0.5821	−0.0790
5	0.0	0.0	0.0	−0.0020	0.0
6			0		
7			0		
⋮					
26			0		
$\sum_{j=1}^{26} =$	0.0052	0.0157	−3.3004	−7.7564	−7.5375

(Table 3 continued)

Au $0.5 < E < \infty$ eV

Group number	Calculation node points (See Fig. 8.)				
	10	17	24	32	40
1	0.0040	0.0047	0.0076	−0.0306	−0.6620
2	0.0201	0.0279	0.0152	−0.1907	−3.7451
3	0.0201	0.0279	−0.0076	−0.2214	−1.3151
4	0.0401	0.0588	0.0385	−0.3728	−1.5622
5	0.0241	0.0471	0.0385	−0.2467	−0.2200
6	0.0201	0.0389	0.0371	−0.1895	−0.0909
7	0.0120	0.0259	0.0318	−0.1185	−0.0303
8	0.0080	0.0227	0.0318	−0.1067	−0.0182
9	0.0040	0.0203	0.0333	−0.1019	−0.0109
10	0.0040	0.0174	0.0334	−0.1093	−0.0054
11	0.0040	0.0174	0.0334	−0.1120	0.0
12	0.0	0.0174	0.0475	−0.1146	0.0
13	−0.0020	0.0174	0.0475	−0.1200	0.0
14	−0.0040	0.0174	0.0523	−0.1316	0.0
15	−0.0060	0.0174	0.0523	0.1400	0.0
16	−0.0080	0.0174	0.0475	−0.1592	0.0
17	−0.0100	0.0116	0.0475	−0.1750	0.0
18	−0.0120	0.0116	0.0190	−0.1911	0.0
19	−0.0140	0.0116	0.0190	−0.1950	0.0
20	−0.0160	0.0929	0.0285	−0.2017	0.0
21	−0.0281	−0.4007	−1.1785	−0.6645	0.0
22	0.0	−0.0436	−0.1331	−0.0786	0.0
23	0.0	−0.0029	−0.0190	−0.0127	0.0
24	0.0	−0.0029	−0.0143	−0.0085	0.0
25	0.0	0.0	0.0	0.0	0.0
26	0.0	0.0	0.0	0.0	0.0
$\sum_{j=1}^{26} =$	0.0604	0.0736	−0.6908	−3.9926	−7.6601

(Table 3 continued)

Au $0 < E < \infty$ eV

Calculation node points (See Fig. 8.)					
Group number	10	17	24	32	40
1	0.0036	0.0	0.0	−0.0036	−0.5977
2	0.0108	0.0091	0.0065	−0.0324	−3.4369
3	0.0108	0.0091	0.0	−0.0443	−1.2765
4	0.0217	0.0229	0.0163	−0.0653	−1.5870
5	0.0108	0.0153	0.0109	−0.0373	−0.2761
6	0.0108	0.0126	0.0135	−0.0283	−0.1271
7	0.0073	0.0063	0.0089	−0.0154	−0.0491
8	0.0036	0.0063	0.0089	−0.0128	−0.0289
9	0.0036	0.0057	0.0081	−0.0115	−0.0181
10	0.0036	0.0057	0.0081	−0.0138	−0.0104
11	0.0036	0.0057	0.0081	−0.0138	−0.0090
12	0.0036	0.0057	0.0121	−0.0115	−0.0078
13	0.0036	0.0057	0.0121	−0.0115	−0.0065
14	0.0036	0.0057	0.0121	−0.0138	−0.0052
15	0.0036	0.0057	0.0121	−0.0138	−0.0039
16	0.0036	0.0057	0.0121	−0.0161	−0.0026
17	0.0	0.0057	0.0121	−0.0161	−0.0026
18	0.0	0.0057	0.0121	−0.0207	−0.0026
19	0.0	0.0057	0.0121	−0.0207	−0.0026
20	0.0	0.0141	0.0161	−0.0230	−0.0026
21	0.0	−0.0339	−0.0886	−0.0737	−0.0026
22	0.0	0.0	0.0040	0.4489	−0.0026
23	0.0	0.0028	0.0121	−0.0046	−0.0026
24	0.0	0.0057	0.0121	−0.0046	−0.0026
25	0.0	0.0057	0.0121	−0.0069	−0.0026
26	0.0495	0.1103	0.1409	−0.7851	−0.0129
$\sum_{j=1}^{26} =$	0.1577	0.2490	0.2948	−1.3042	−7.4791

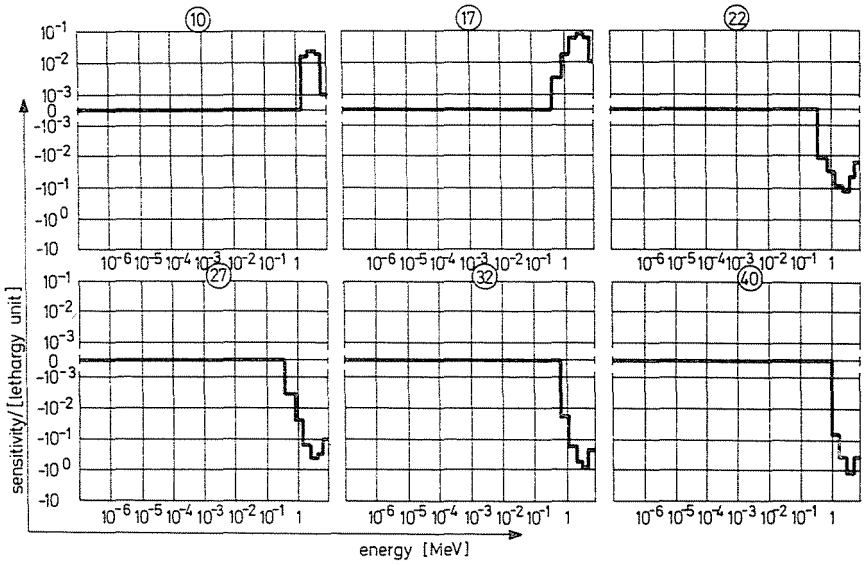

Fig. 5. Sensitivity profile of reaction rate
Configuration 1 (In $E > 1$ MeV)

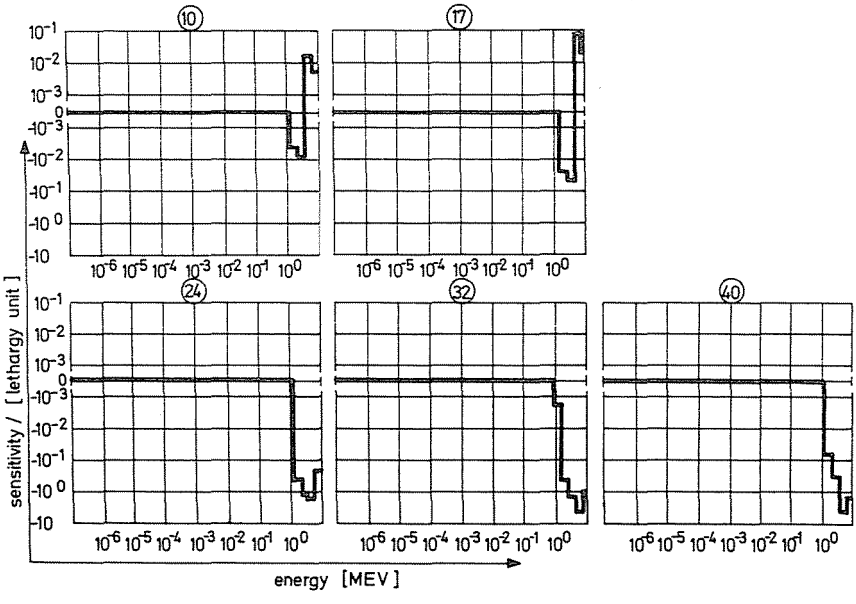

Fig. 6. Sensitivity profile of reaction rate
Configuration 2 (S $E > 3$ MeV)

These figures demonstrate that in the entire thickness of the shield layer (30 cm for water and 42.7 cm for graphite) the sensitivity is of linear characteristics; the curves subsequently deviate due to the change in the composition of the shield.

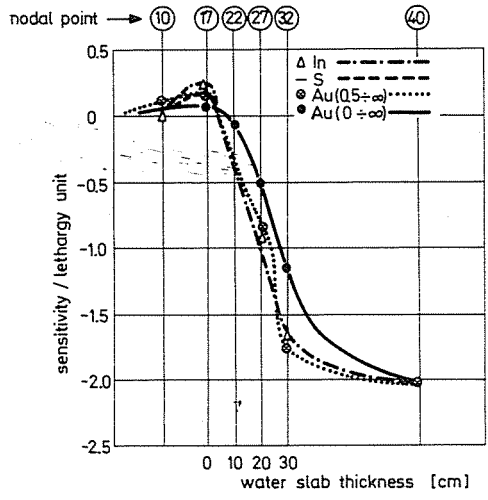

Fig. 7. Total sensitivity in terms of the shield thickness. Configuration 1

This linear dependence of sensitivity on the shield thickness enables the curve to be extrapolated for greater thicknesses. In the case of oxygen (water-shield, Fig. 7) it can be seen that, for example, extrapolating for 1.5 m water thickness, the total sensitivity has a value of about 10. This means that if the calculation is carried out with cross section data of an accuracy of say 5%, the integral quantity will be obtained with an accuracy of 50%. This already exceeds the error of the removal-diffusion calculation method. In the case of carbon (graphite-shield, Fig. 8) the extrapolation shows that the uncertainty of the cross section exceeds the error of the calculation method at 40 cm graphite thickness.

It can thus be seen that for large shield thicknesses the oxygen and carbon cross section data in the ABBN data set used for the removal-diffusion calculation method need correction.

It is emphasized that the sensitivity analysis used for the shielding problem described in the present paper was not aimed at prescribing an accuracy requirement for the cross sections examined and promoting thereby a better agreement between the calculated and measured reactor quantities by the more accurate cross section data fitted in integral experiments.

Our purpose was to show that in biological shield calculations, approaching sensitivity analysis from another side, the results can be utilized in order to set limits for the quantitative and qualitative conditions of the validity of the data set in the calculations.

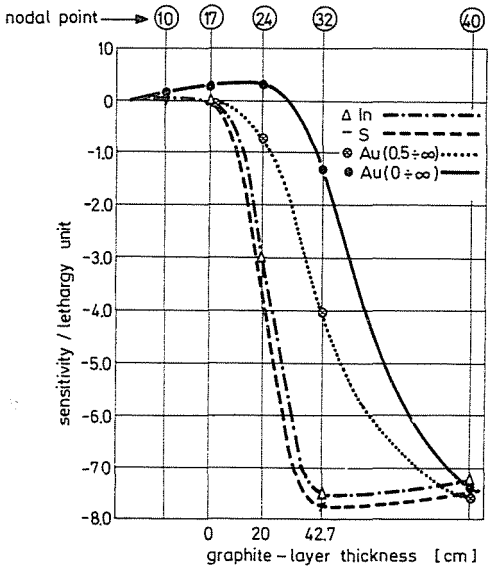

Fig. 8. Total sensitivity in terms of the shield thickness. Configuration 2

Acknowledgements

Helps of the leaders and all the staff of Department of Nuclear Power Station of Energetical University of Moscow are acknowledged by author for their kind support.

Special thanks are due to professor T. H. Margulova for her encouraging help and many discussions within the subject and to professor N. G. Volkov and to first assistent, to professor G. G. Bartolomej for their guidance in the scientific matter.

Summary

The approach of the sensitivity analysis problem described in the present paper is shown to be an effective method for biological shield calculation to determine reactor quantities obtained from integral experiments. However, it must be borne in mind that in this case the integral experiments that can be carried out are more limited than in the case of core measurements.

It is obviously somewhat risky to extrapolate the obtained results for all shield-designing requirements, based on the sensitivity analysis of a particular data set, since sensitivities are extremely problem-dependent in shield calculations.

This notwithstanding, the results presented here prove that at a certain stage of shield design, reliable and relatively rapid information can be obtained on the accuracy of a reactor quantity measured in a relatively undemanding integral experiment and calculated by a well-tested code, based on a semi-empirical calculation procedure using the method of cross section sensitivity analysis proposed here.

References

1. CECCHINI, G.—FARINELLI, U.—GANDINI, A.—SALVATORES, M.: Analysis of integral data for few group parameter evaluation of fast reactors. A/Conf. 28/P/627, Geneva (1964).
2. CECCHINI, G.—GANDINI, A.: Comparison between Experimental Integral Data on Fast Critical Facilities. ANL-7320, p. 107. Argonne (1966 October).
3. BAKER, A. R.: Comparative Studies of the Criticality of Fast Critical Assemblies. ANL-7320, p. 116. Argonne (1966 October).
4. BAKER, A. R.: International Conference on Fast Reactor Physics. BNES, October 1969, Volume 8, Number 4, p. 253.
5. HÄGGBLOM, H.: Adjustment of Neutron Cross Section Data by a Least Square Fit of Calculated Quantities to Experimental Results. AE-422 (Aktiebolaget Atomenergi) 1971 May.
6. CAMPBELL, C. G.—ROWLANDS, J. L.: The relationship of microscopic and integral data. Proc. of IAEA Conf. on Nuclear Data for Reactors, Helsinki, 1970. Vol. II. pp. 391—425. IAEA-CN-26/116.
7. MITANI, H.—KUROI, H.: Adjustment of Group Cross Sections by Means of Integral Data. Part I., Part II. J. of Nuclear Sciense and Technology, Volume 9, Number 7. July 1972 p. 383–394 és Volume 9, Number 11, November 1972, p. 642–657.
8. PENDLEBURY, E. D.: Critical Experiments and Spectrum Measurements on The Validity of Microscopic Data. Proceedings of The Third Conference Neutron Cross Section and Technology, March, 1971 Knoxville, Tennessee. CONF. 71031 (Vol. 1) p. 1–25.
9. PAZY, A.—RAKAVY, G.—REISS, I.—WAGSCHAL, J. J.: The Role of Integral Data in Neutron Cross. Section Evaluation. Nuclear Science and Eng.: **55**, 280–295 (1974).
10. WAGSCHAL, J. J.—YEIVIN, Y.: Differential Cross Section and Integral Data: the ENDF/B-4 Library and "Clean" Criticals.
11. GOLDSTEIN, H.: A Survey of Cross Section Sensitivity Analysis as Applied to Radiation Shielding. Proceedings of the Fifth International Conference on Reactor Shielding. Knoxwille, Tennessee, USA. April, 1977.
12. "Результаты измеренний тестовой программы № 2. по биологической зашите". Реп. БТУ-УР-61/1977. Будапешт. Тема 1-4.3.1. СЭВ. Под. ред. Чом Д.
13. АБАГЯН, Л. П.—БАЗАЗЯНЦ, И. И.—БОНДАРЕНКО, М. Н.—НИКОЛАЕВ, Х. И.: "Групповые константы для расчета ядерных реакторов." Москва, Атомиздат, 1964.
14. WEINBERG, A. M.—WIGNER, E. P.: "The Physical Theory of Neutron Chain Reactors". The Univ. of Chicago Press, Chicago. Third Impression, 1972.
15. ALBERT, R. D.—WELTON, T. A.: A Simplified Theory on Neutron Attenuation and Its Application to Reactor Shield Design. USAEC, Rep. WARD-15. 1950.
16. БЕРГЕЛСОН, В. Р.—ЧУПРАКОВ, Д. В.: Многогрупповая программа расчета одномерной защиты от нейтронов. В кн. "Радиационная безопасность и зашита АЭС". Сборник стат. под ред. Ю. А. Егорова и др. Вып. 2. Москва, Атомиздат, 1976. стр. 156.
17. Михай, К.: Использование метода выведения-диффузии для расчета тестовой программы по биологической защите. В сб.: Трудов МЭИ. Теплогидравлические и физико-химические процессы в ядерных установках. Вып. 474. стр. 59–64 Москва, 1980.
18. Михай, К.: Использование интегральных кинетических уравнений для расчета многослойных защит. В сб. Трудов МЭИ. Теплогидр. и физ. хим. процессы в ядерных энергетических установках. Вып. 474. стр. 65–74, Москва 1980.
19. Михай, К.: Использование интергальных экспериментов с целью анализа ядерных констант для расчета биологической защиты ядерных реакторов. Кандидатская диссертация, Москва, 1980.
20. WIGNER, E. P.: Effect of Small Perturbation on Pile Period. Chicago Report CP-G-3048, 1945.

21. Усачев, Л. Н.: Уравнение для ценности нейтронов, кинетика реактора и теория возмущений. Труды 1. Женевской Конференции, 5P/616. 1955.
22. Марчук, Г. И.: "Методы расчета ядерных реакторов" Москва, Атомиздат 1961.
23. Усачев, Л. Н.: Теория возмущений для коэффициента воспроизводства и других отношений чисел различных процессов в реакторе. Атомная Энергия, 1963, № 12. 427–481.
24. Усачев, Л. Н.: Математическая теория эксперимента и обобщенная теория возмущений-эффективный подход к исследованию физики реакторов. Ядерные Константы. Вып. 10. Атомиздат, 1972 стр. 3–12.
25. Oblow, E. M.: The Sensitivity Analysis Development and Applications Program at ORNL. Proc. of the Specialists' Meeting on Sensitivity Studies and Shielding Benchmarks. Paris, 1975, pp. 38–47.
26. Михай, К.: Анализ чувсвительности ядерных констант для инженерных методов расчета биологической защиты ядерных реакторов. Доклад на конф:"Нейтронной физики", Киев, 15–19, сентября 1980.

Dr. Kate Mihály H-1521 Budapest